National Defence / Défense nationale

UNCLASSIFIED
UNLIMITED DISTRIBUTION

(1)

CREV REPORT 469293
JANUARY 1993

CRDV RAPPORT 469293
JANVIER 1993

BRIDGING THE GAP BETWEEN THE RAYLEIGH AND THOMSON LIMITS FOR VARIOUS CONVEX BODIES

G.R. Fournier

B.T.N. Evans

RESEARCH AND DEVELOPMENT BRANCH
DEPARTMENT OF NATIONAL DEFENCE
CANADA

BUREAU - RECHERCHE ET DÉVELOPPEMENT
MINISTÈRE DE LA DÉFENSE NATIONALE
CANADA

Defence Research Establishment
Centre de recherches pour la Défense,
Valcartier, Québec

Canada

SANS CLASSIFICATION
DISTRIBUTION ILLIMITEE

BRIDGING THE GAP BETWEEN THE RAYLEIGH AND THOMSON LIMITS FOR VARIOUS CONVEX BODIES

by

G.R. Fournier and B.T.N. Evans

DEFENCE RESEARCH ESTABLISHMENT

CENTRE DE RECHERCHES POUR LA DÉFENSE

VALCARTIER

Tel: (418) 844-4271

Québec, Canada January/janvier 1993

ABSTRACT

It is well known that the Rayleigh approximation to extinction, scattering and absorption efficiencies for spheres is limited to small size parameters, x, and small values of $|m|x$, where m is the complex index of refraction. It is also known that the Thomson approximation to these same efficiencies is valid for small x and $m = \infty$. We have established an exact transform of the Mie coefficients, for both spheres and infinite cylinders, that removes the m related restrictions of the Rayleigh and Thomson approximations. The resulting series for spheres and infinite cylinders are valid for all m and small x. This transform can also be applied in an approximate form to spheroids.

RÉSUMÉ

L'approximation de Rayleigh pour l'efficacité d'extinction, de diffusion et d'absorption des sphères est limitée aux petites valeurs du paramètre de taille, x, et aux petites valeurs de $|m|x$, m étant l'indice de réfraction complexe. L'approximation de Thomson est de son coté valide pour les petites valeurs de x et $m = \infty$. Nous avons établi une transformation exacte des coefficients de Mie pour les sphères et les cylindres infinis qui fait disparaître ces restrictions sur la valeur de m dans les approximations de Thomson et Rayleigh. La série qui en résulte est valide pour tout m, x demeurant petit. Cette transformation peut aussi s'appliquer aux sphéroïdes mais d'une manière approximative.

TABLE OF CONTENTS

EXECUTIVE SUMMARY

Any complex military system or scenario that involves electro-optical devices requires understanding the propagation of radiation through natural aerosols and smokes/obscurants. Given present and future electro-optical capabilities of fire-control systems, full spectrum obscurants will be required as effective countermeasures. It is well known that spherical particles obscure efficiently in the visible region of the spectrum. It is also well known that, in the near and far infrared, as well as the microwave region of the spectrum, the use of nonspherical particles is mandatory. The most efficient obscurants generally require that the obscuring particles be made from highly refractive materials (for example, metals).

This work considers the calculation of the extinction efficiency from small, nonspherical particles (by small particles we mean that the particle size is small relative to the wavelength). It has two main objectives. The first is to extend the calculation to previously inaccessible parameter domains and the second is to significantly reduce the computational burden. This would allow the full exploration of the effects of these particles on the performance of obscurants and on electromagnetic propagation.

To date the theoretical exploration of the effect of these types of particles on the performance of obscurants has been either extremely restrictive or prohibitively expensive. This work partially overcomes these restrictions and will aid in the design and performance analysis of potential new obscurants using high-refractivity materials.

The electromagnetic extinction through rain, carbon smoke or other nonspherical atmospheric aerosols can also be evaluated by this approach. This is an essential first step in the evaluation of the performance of all electro-optical systems.

The long-term goal of this work is to alleviate the remaining constraints in the theoretical consideration of nonspherical aerosols and obscurants of both natural and artificial origin. This will not only aid in finding better obscurants but also in the possible identification and remote classification of such aerosols.

1.0 INTRODUCTION

If a particle is geometrically and optically small enough, then simple formulae can usually be found for the extinction and scattering efficiencies as well as the phase function. Such approximate formulae are usually called the Rayleigh approximation (Refs. 1 and 2). If the particle is still geometrically small but optically very large, the Thomson approximation results (Ref. 3). Often, however, a geometrically small particle may be neither optically small nor very large. This creates a gap that has not been completely filled.

In this report we first demonstrate a transform that bridges this gap for spheres and infinite cylinders. If this transform of the Mie coefficients and their series expansion were limited to spheres and infinite cylinders, it would have only theoretical interest. However, this transform generalizes, in an approximate form, to other convex bodies when a Rayleigh or Thomson-like series can be obtained. These can sometimes be obtained by a method given by Stevenson in 1953 (Ref. 4). Series are available in this document for ellipsoids (which include spheroids). We will present results of a comparison between the newly obtained series and the exact codes for spheres and spheroids.

This work was performed at DREV between March and October 1991 under PSC 32A, EO/IR Protection of Land Vehicles.

2.0 THEORY

We will first derive the general expansion of the Mie coefficients for small size parameters x, and show how the Rayleigh and Thomson expressions result.

2.1 Spheres

Starting with the definition (Ref. 2) of Q_{sca} and Q_{ext}, the scattering and extinction efficiencies, respectively, we have

$$Q_{sca} = \frac{2}{x^2}\sum_{n=1}^{\infty}(2n+1)\{|a_n|^2 + |b_n|^2\}, \qquad [1]$$

and

$$Q_{ext} = \frac{2}{x^2}\sum_{n=1}^{\infty}(2n+1)\{\mathrm{Re}(a_n + b_n)\}, \qquad [2]$$

where a_n and b_n are the external field Mie coefficients. These Mie coefficients are given by

$$a_n = \frac{\sqrt{\mu}\,\psi_n'(\sqrt{\epsilon\mu}\,x)\,\psi_n(x) - \sqrt{\epsilon}\,\psi_n(\sqrt{\epsilon\mu}\,x)\,\psi_n'(x)}{\sqrt{\mu}\,\psi_n'(\sqrt{\epsilon\mu}\,x)\,\zeta_n(x) - \sqrt{\epsilon}\,\psi_n(\sqrt{\epsilon\mu}\,x)\,\zeta_n'(x)}, \qquad [3]$$

and

$$b_n = \frac{\sqrt{\epsilon}\,\psi_n'(\sqrt{\epsilon\mu}\,x)\,\psi_n(x) - \sqrt{\mu}\,\psi_n(\sqrt{\epsilon\mu}\,x)\,\psi_n'(x)}{\sqrt{\epsilon}\,\psi_n'(\sqrt{\epsilon\mu}\,x)\,\zeta_n(x) - \sqrt{\mu}\,\psi_n(\sqrt{\epsilon\mu}\,x)\,\zeta_n'(x)}, \qquad [4]$$

where ϵ and μ are the relative dielectric constant and the relative magnetic permeability, ψ_n is the Riccati-Bessel function of the first kind and ζ_n is the Riccati-Bessel function of the third kind. Note that the b_n coefficients are symmetrical with the a_n coefficients upon substitution of ϵ for μ and vice versa. Hence, we need only discuss a_n in detail.

Expanding a_1 and a_2 in small x we obtain

$$a_1 = \frac{2}{3}i\left(\frac{\epsilon-1}{\epsilon+2}\right)x^3 + \frac{1}{5}i\left(\frac{\epsilon^2-6\epsilon+4+\epsilon^2\mu}{(\epsilon+2)^2}\right)x^5 + \frac{4}{9}\left(\frac{\epsilon-1}{\epsilon+2}\right)^2 x^6$$
$$+\frac{1}{175}i\left(\frac{\epsilon^4\mu^2+\epsilon^3(9\mu^2+35\mu-25)-\epsilon^2(70\mu+150)+200(2\epsilon-1)}{(\epsilon+2)^3}\right)x^7+\ldots, \qquad [5]$$

$$a_2 = \frac{1}{15}i\left(\frac{\epsilon-1}{2\epsilon+3}\right)x^5+\ldots, \qquad [6]$$

$$b_n = a_n,\ \epsilon \leftrightarrow \mu.$$

Expansions for higher order coefficients can also be derived. The classic Rayleigh approximation gives ($\mu = 1$, $m^2 = \epsilon\mu$),

$$a_1 = \frac{2}{3}i\left(\frac{m^2-1}{m^2+2}\right)x^3 + \frac{2}{5}i\left(\frac{(m^2-1)(m^2-2)}{(m^2+2)^2}\right)x^5 + \frac{4}{9}\left(\frac{m^2-1}{m^2+2}\right)^2 x^6$$
$$+\frac{1}{175}i\left(\frac{(m^2-1)(m^6+20m^4-200m^2+200)}{(m^2+2)^3}\right)x^7+\ldots, \qquad [7]$$

$$b_1 = \frac{1}{45}i(m^2-1)x^5+\ldots. \qquad [8]$$

The Thompson approximation gives ($\epsilon \to \infty$, $\mu = 0$),

$$a_1 = \frac{2}{3}ix^3 + \frac{1}{5}ix^5 + \frac{4}{9}x^6 - \frac{1}{7}ix^7+\ldots, \qquad [9]$$

$$b_1 = -\frac{1}{3}ix^3 + \frac{1}{5}ix^5+\ldots. \qquad [10]$$

It is immediately apparent that as $m \to \infty$ the Rayleigh expansion for either a_1 or b_1 does not converge even for small values of x. Hence, the requirement for *small optical size* $|mx|$. The Thomson expansion, having no index dependency, applies only to infinite optical size. The problem with the Rayleigh series mathematically arises from the terms in a_n with $\epsilon^2\mu$ and in b_n with $\mu^2\epsilon$. If these terms were set to zero, the divergence problem would disappear. We must, however, recover the lost information without reintroducing the divergence problem.

To do this rewrite a_n to isolate the material properties as

$$a_n = \frac{\psi_n(x) - \left\{ \frac{\sqrt{\epsilon}\,\psi_n(\sqrt{\epsilon\mu}\,x)}{\sqrt{\mu}\,\psi_n'(\sqrt{\epsilon\mu}\,x)} \right\} \psi_n(x)}{\zeta_n(x) - \left\{ \frac{\sqrt{\epsilon}\,\psi_n(\sqrt{\epsilon\mu}\,x)}{\sqrt{\mu}\,\psi_n'(\sqrt{\epsilon\mu}\,x)} \right\} \zeta_n'(x)}. \qquad [11]$$

Consider the result of letting $\mu \to 0$ in the above expression (which will make all the $\epsilon^2\mu$ terms zero along with others),

$$\lim_{\mu \to 0} a_n = \frac{\psi_n(x) - \left\{ \frac{\epsilon\, x}{n+1} \right\} \psi_n'(x)}{\zeta_n(x) - \left\{ \frac{\epsilon\, x}{n+1} \right\} \zeta_n'(x)}. \qquad [12]$$

To recover the full Mie coefficients, replace ϵ in the above limit by

$$\epsilon \to \frac{\sqrt{\epsilon}}{\sqrt{\mu}} \frac{(n+1)}{x} \frac{\psi_n(\sqrt{\epsilon\mu}\,x)}{\psi_n'(\sqrt{\epsilon\mu}\,x)} = \mathcal{E}_n, \qquad [13]$$

and by symmetry,

$$\mu \to \frac{\sqrt{\mu}}{\sqrt{\epsilon}} \frac{(n+1)}{x} \frac{\psi_n(\sqrt{\epsilon\mu}\,x)}{\psi_n'(\sqrt{\epsilon\mu}\,x)} = \mathcal{U}_n. \qquad [14]$$

Both $\mathcal{E}_n$ and $\mathcal{U}_n$ can be considered as transformed material properties. Putting these new variables back into [12] and expanding in small x, *as if* $\mathcal{E}_n$ *and* $\mathcal{U}_n$ *were independent of* x,

we obtain,

$$a_1 = \frac{2}{3}i\left(\frac{\mathcal{E}_1 - 1}{\mathcal{E}_1 + 2}\right)x^3 + \frac{1}{5}i\left(\frac{\mathcal{E}_1^2 - 6\mathcal{E}_1 + 4}{(\mathcal{E}_1 + 2)^2}\right)x^5 + \frac{4}{9}\left(\frac{\mathcal{E}_1 - 1}{\mathcal{E}_1 + 2}\right)^2 x^6$$

$$-\frac{1}{7}i\left(\frac{\mathcal{E}_1^3 + 6\mathcal{E}_1^2 - 16\mathcal{E}_1 + 8}{(\mathcal{E}_1 + 2)^3}\right)x^7 + \ldots, \qquad [15]$$

$$a_2 = \frac{1}{15}i\left(\frac{\mathcal{E}_2 - 1}{2\mathcal{E}_2 + 3}\right)x^5 + \ldots, \qquad [16]$$

and again by symmetry,

$$b_n = a_n, \ \mathcal{E}_n \leftrightarrow \mathcal{U}_n.$$

Note singularities occur if and only if

$$\mathcal{E}_n = -(n+1)/n, \qquad [17]$$

and

$$\mathcal{U}_n = -(n+1)/n, \qquad [18]$$

which requires a real ϵ (or real μ). For all other values of $\mathcal{E}$ and $\mathcal{U}$ the coefficients of series [15] and [16] are finite to all orders of x. Thus [15] and [16] are valid for all nonreal values of the refractive index. However, when the conditions [17] and [18] are nearly satisfied, many terms in [15] and [16] will be required before the series converges to a given accuracy. For convenience in computations we can rewrite $\mathcal{E}_n$ as,

$$\mathcal{E}_1(z) = -\frac{2\epsilon F}{(1+F)}, \ \mathcal{E}_2(z) = -\frac{3\epsilon(1+3F)}{2+6F-Fz^2} \ \ldots, \qquad [19]$$

with

$$F(z) = \frac{z\cot(z) - 1}{z^2}, \text{ and } z = \sqrt{\epsilon\mu}x = (n - ik)x, \qquad [20]$$

and

$$\mathcal{U}_n = \mathcal{E}_n, \epsilon \rightarrow \mu.$$

Since the 'Mie' coefficients for the normal incidence infinite cylinder (Ref. 2) are identical to the sphere Mie coefficients, apart from the order of the Bessel functions involved, the same procedure can be used to obtain a series for small particles independent of material properties. Oblique incidence can also be done but generates much more complicated expressions.

2.2 Spheroids

The above series [15] etc. by itself is interesting only from the classic nature of the Rayleigh and Thomson series. However, the idea of transforming a Rayleigh-like series, (with the optical size constraint) into a series that is independent of the material properties, for many types of regular particle shapes, would be of practical use. We show here that this can be achieved, to some approximation, with oriented and randomly oriented spheroids.

The Rayleigh approximation (with arbitrary μ) for oriented spheroids (Refs. 4 and 5), Q_{ray}, is given by

$$Q_{ray} = Q_{sca} + Q_{abs}, \qquad [21]$$

where

$$Q_{sca} = \frac{8}{3}\frac{b^4 r^2}{p}\left\{\frac{\sin^2\theta}{2}\left(|\eta_1|^2 + |\eta_1'|^2\right) + \frac{(1+\cos^2\theta)}{2}\left(|\eta_2|^2 + |\eta_2'|^2\right)\right\}, \qquad [22]$$

$$Q_{abs} = 4\frac{br}{p}\,\mathrm{Re}\Big\{i\Big[\frac{\sin^2\theta}{2}\,(\eta_1 + \eta_1') + \frac{(1+\cos^2\theta)}{2}\,(\eta_2 + \eta_2')\Big]\Big\}, \qquad [23]$$

and where

$$p = \sqrt{\cos^2\theta + r^2\sin^2\theta}, \qquad a = 2\pi\alpha/\lambda, \qquad b = 2\pi\beta/\lambda. \qquad [24]$$

Here $r = a/b$ is the aspect ratio (for prolates $r > 1$ and for oblates $r < 1$), α is the length of the semi-axis of rotation, β is the other semi-axis of the spheroid, θ is the angle between the incident radiation and the α (or a axis), and λ is the wavelength of the scattered radiation. Furthermore,

$$\eta_1 = \frac{1}{3(L_1 + \frac{1}{\epsilon-1})} \quad \text{and} \quad \eta_1' = \frac{1}{3(L_1 + \frac{1}{\mu-1})}, \qquad [25]$$

$$\eta_2 = \frac{1}{3(L_2 + \frac{1}{\epsilon-1})} \quad \text{and} \quad \eta_2' = \frac{1}{3(L_2 + \frac{1}{\mu-1})}, \qquad [26]$$

and the form factors are defined for prolates (i.e. $r > 1$) as

$$L_1 = \frac{(1-g^2)}{g^2}\Big\{-1 + \frac{1}{2g}\ln\Big(\frac{1+g}{1-g}\Big)\Big\}, \qquad [27]$$

$$L_2 = \frac{1-L_1}{2}, \qquad [28]$$

$$g^2 = 1 - \frac{1}{r^2}. \qquad [29]$$

For oblates (i.e. $r < 1$) we have

$$L_1 = \frac{1+f^2}{f^2}\Big\{1 - \frac{\tan^{-1} f}{f}\Big\}, \qquad [30]$$

$$L_2 = \frac{1-L_1}{2}, \qquad [31]$$

$$f^2 = \frac{1}{r^2} - 1. \qquad [32]$$

Normally, $\mu = 1$ in the above equations and hence η_1' and η_2' are both zero. The procedure, as demonstrated for spheres, requires the full expression for the efficiencies, therefore we retain the μ terms.

Since the scattered wave at large distances from finite convex bodies can be approximated by a series of Riccati-Bessel functions, we will use the same material transforms, [13] and [14], but with the arguments modified. Furthermore these transforms will be angle independent to first order. This can be understood by considering that the first mode can be excited in any resonant phenomena without regard to the direction of the triggering energy. This is readily verified by using an exact infinite cylinder scattering code.

The modification is simply an approximation to the effective optical size, $\overline{z}$, of the spheroid. We want a simple formula that will give the sphere material transform when $r = 1$ and gives the emipirically derived asymptotes (of $\overline{z}/b$) as either $r \to \infty$ or $r \to 0$. It can be shown formally (Refs. 7 and 8) that the η_1 and η_2 terms come from different vector spheroidal wavefunctions. This implies that we will have, for either prolates or oblates, two different expressions for $\overline{z}$. Using the T-matrix method (Ref. 6) we have empirically derived the following expressions:

$$\overline{z} = \left.\begin{array}{ll} \sqrt{\epsilon\mu}\, b\,(1 + \nu\,(1 - 1/r^2)) & \text{prolates} \\ \sqrt{\epsilon\mu}\, b\,(r^2)^{\nu} & \text{oblates} \end{array}\right\} \quad \text{for } \eta_1, \text{ and} \qquad [33]$$

$$\overline{z} = \left.\begin{array}{ll} \sqrt{\epsilon\mu}\, b\,(1 + \nu^{1/3}(1 - 1/\sqrt{r})) & \text{prolates} \\ \sqrt{\epsilon\mu}\, b\,(\sqrt{r})^{\nu^{1/}} & \text{oblates} \end{array}\right\} \quad \text{for } \eta_2 \qquad [34]$$

where $\nu \approx \sqrt{3}/10$.

It is found, when [33] and [34] are used in the final formalism, the positions of the first two polaritons are well modelled from $0.1 \leq r \leq 20$.

For randomly oriented spheroids the cross sections C_{sca} and C_{abs} must be integrated over all angles. C_{sca} is just [22] multiplied by $\pi p b^2$ and similarly for C_{abs} from [23]. The efficiencies are then obtained, in the usual way, by normalizing the cross sections by the average projected area. The integration is simple since η_1, η_1', η_2 and η_2' are independent of the orientation angle. Replacing ϵ with $\mathcal{E}_1(\bar{z})$ and μ with $\mathcal{U}_1(\bar{z})$, integrating C_{sca} and C_{abs} over $\sin(\theta)\, d\theta$ from 0 to $\pi/2$ and then normalizing we get

$$\overline{Q}_{sca} = \frac{16}{9}\frac{b^4 r^2}{\overline{A}}\left\{|\tilde{\eta}_1|^2 + |\tilde{\eta}_1'|^2 + 2\left(|\tilde{\eta}_2|^2 + |\tilde{\eta}_2'|^2\right)\right\}, \qquad [35]$$

and

$$\overline{Q}_{abs} = \frac{8}{3}\frac{br}{\overline{A}}\mathrm{Re}\left\{i\left[\tilde{\eta}_1 + \tilde{\eta}_1' + 2\left(\tilde{\eta}_2 + \tilde{\eta}_2'\right)\right]\right\}, \qquad [36]$$

where the normalization factor is, for prolates,

$$\overline{A} = 1 + \frac{r^2}{\sqrt{r^2-1}}\sin^{-1}\left(\frac{\sqrt{r^2-1}}{r}\right), \qquad [37]$$

and for oblates,

$$\overline{A} = 1 + \frac{r^2}{\sqrt{1-r^2}}\ln\left(\frac{1+\sqrt{1-r^2}}{r}\right), \qquad [38]$$

and

$$\tilde{\eta}_1 = \frac{1}{3(L_1 + \frac{1}{\mathcal{E}_1 - 1})}, \quad \tilde{\eta}_1' = \frac{1}{3(L_1 + \frac{1}{\mathcal{U}_1 - 1})}, \qquad [39]$$

$$\tilde{\eta}_2 = \frac{1}{3(L_2 + \frac{1}{\mathcal{E}_1 - 1})}, \quad \tilde{\eta}_2' = \frac{1}{3(L_2 + \frac{1}{\mathcal{U}_1 - 1})}. \qquad [40]$$

Remember that in the expressions for $\mathcal{E}_1$ and $\mathcal{U}_1$, [13] and [14], $\sqrt{\epsilon\mu}x$ must be replaced by $\bar{z}$.

3.0 RESULTS OF COMPARISON

In this chapter we will demonstrate the accuracy and utility of the expressions and ideas in the preceding chapter. First, we will discuss the comparison of the Rayleigh [7], Thomson [9] and our new series [15] with the exact Mie solution.

Figure 1 shows the three series normalized by the Mie calculation as a function of size parameter. The series for Q_{sca} are calculated to fourth order in x and for a refractive index of $500 - 500i$ which corresponds to metals in the millimeter wave region. When $|mx|$ is small both the Rayleigh and the new series are excellent approximations. As expected the Thomson series overestimates Q_{sca} by 25%. The situation reverses when $|mx|$ is very large. Now the Rayleigh series underestimates Q_{sca} by 25%. Note, however, that in the intermediate range of $|mx|$, [15] is still excellent.

The next figure, Fig. 2, shows, for the same index as above, the comparison of the Mie solution of Q_{ext} with the new approximation and the Rayleigh series. Now the discrepancies between Rayleigh and Mie are quite obvious. This large discrepancy is obviously due to absorption (for more details, see Ref. 1, p. 292). This effect is well modelled by the new series.

To show that [15] adequately models resonances we now choose an index with a large real part and small imaginary or absorptive component. Figure 3 is a diagram of Q_{ext} as calculated by Mie theory and the new series [15] to fourth order, for an index of

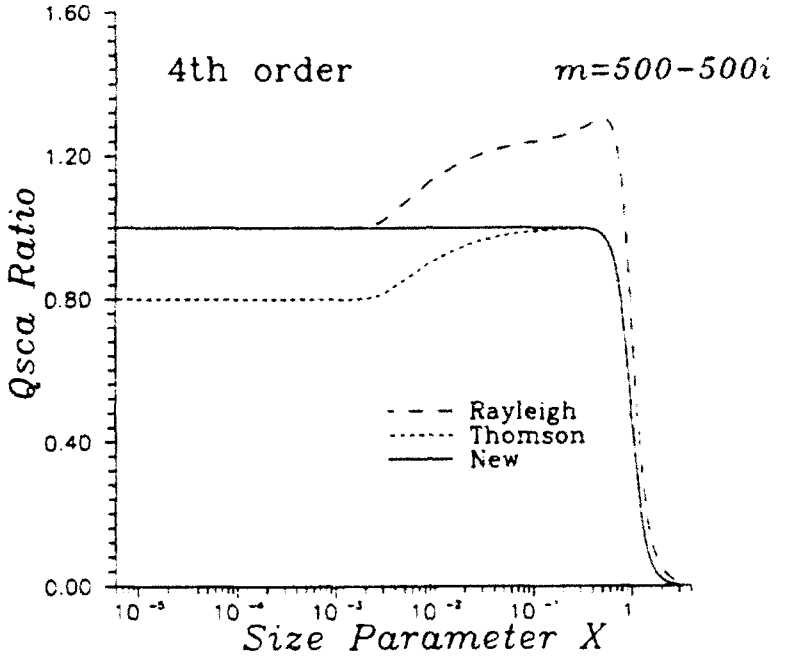

FIGURE 1 – Three series for Q_{sca} normalized by the Mie calculation, as a function of size parameter. Refractive index $m = 500 - 500i$.

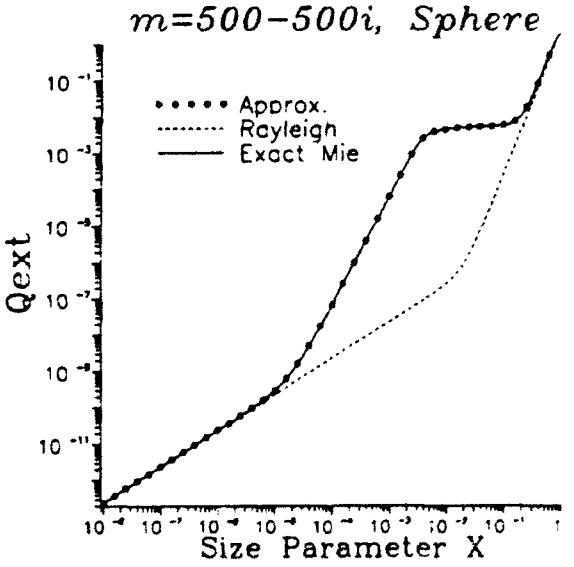

FIGURE 2 – Q_{ext} as calculated by Mie theory, the new series [15] and Rayleigh. Refractive index $m = 500 - 500i$.

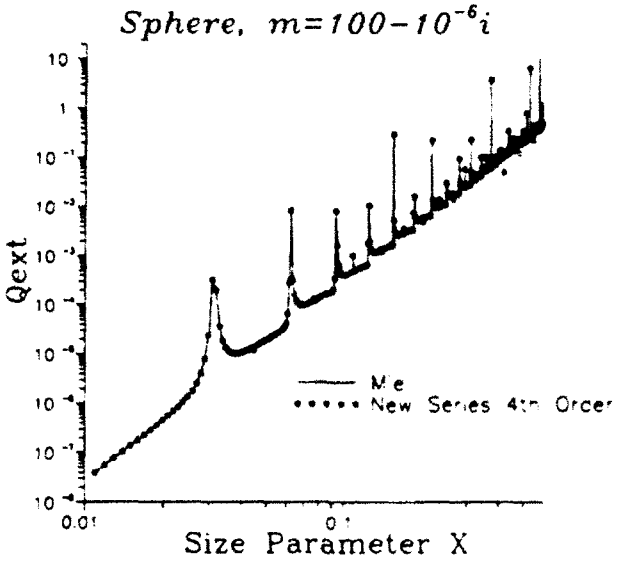

FIGURE 3 – Q_{ext} as calculated by Mie theory and the new series [15] for an index of $100 - 10^{-6}$i.

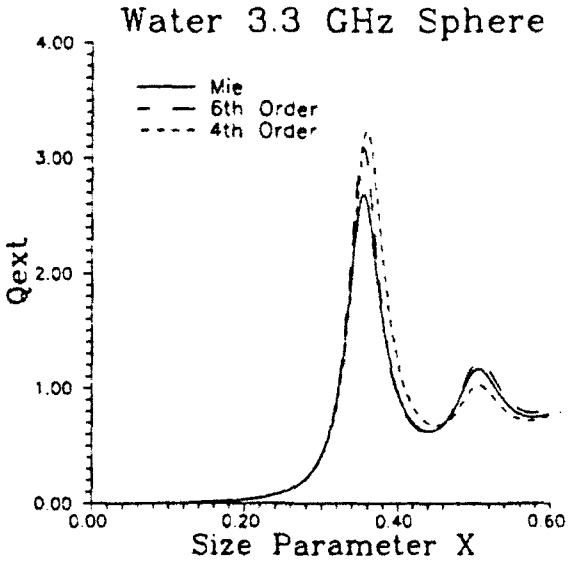

FIGURE 4 – Q_{ext} for water spheres at 3.3 GHz. Refractive index $m = 8.743 - 0.6409$i.

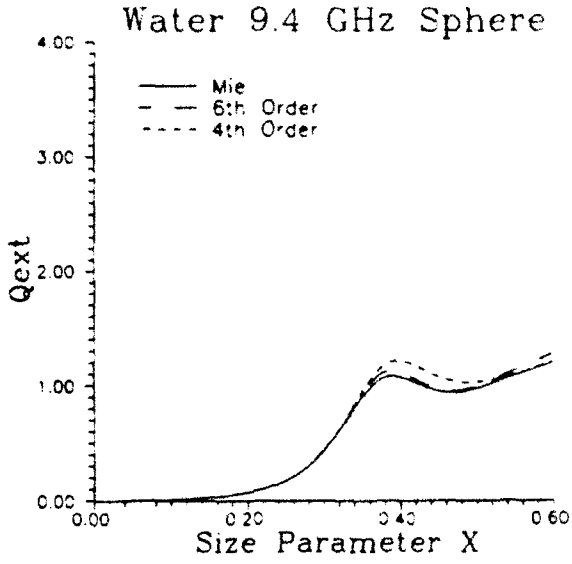

FIGURE 5 – Q_{ext} for water spheres at 9.4 GHz. Refractive index $m = 8.075 - 1.824i$.

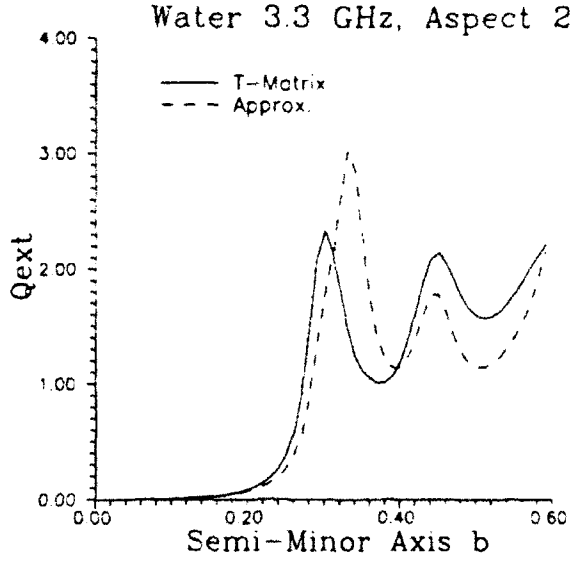

FIGURE 6 – Q_{ext} for water spheroids, $r = 2$, at 3.3 GHz. Refractive index $m = 8.743 - 0.6409i$.

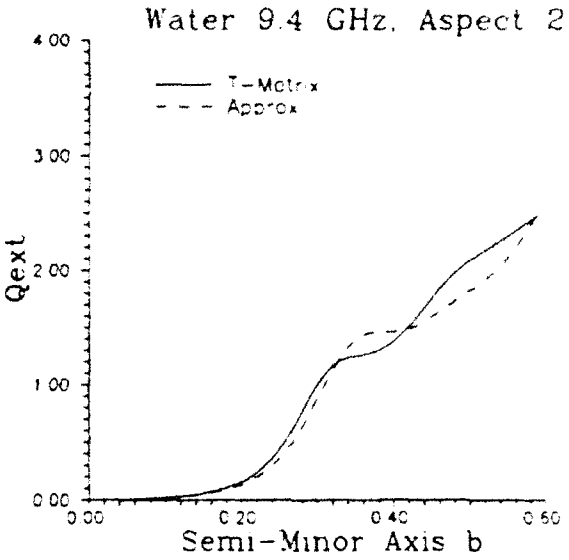

FIGURE 7 – Q_{ext} for water spheroids, $r = 2$, at 9.4 GHz. Refractive index $m = 8.075 - 1.824i$.

$100 - 10^{-6}i$. Although this index is extreme and not physical, it is used here to demonstrate that [15] is still valid for such unusual cases. This emphasizes that [15] applies to arbitrary indices for small x. Notice that not all resonances are modelled. This is because the higher order Mie coefficients, a_n and b_n where $n > 1$, have not been used in this approximation of Q_{ext}.

The effect of using the sixth order expansion instead of the fourth order one can be seen in Figs. 4 and 5. The cases are Q_{ext} for water at 3.3 GHz and 9.4 GHz, respectively. It can be seen that the sixth order corrects for both amplitude and skewness around the resonances. Evidently, higher order expansion would improve the accuracy further. It is interesting that the fourth order captures most of the detail, even around the resonances.

Figures 6 and 7 are the same cases as for the previous two diagrams except that prolate spheroids, with an aspect ratio 2, are considered instead of spheres. The exact calculations are performed using the T-Matrix method (Ref. 6). Also the size parameter x has been replaced by the semi-minor axis b. As expected, the features are similar but many significant changes can be observed. Relative amplitudes and locations of the resonances have changed as well as the underlying trend in the curves. The agreement, while not excellent, is still remarkable because of the simplicity of the series compared with the exact calculation for such a large optical size. This large optical size almost makes the T-matrix ill-conditioned. No such problem occurs for the series.

Figures 8 and 9 are similar to Figs. 6 and 7 but now oblate spheroids of aspect 0.5 are considered. The results are similar to the prolate cases for both Q_{ext} and the degree of agreement between the T-Matrix calculation and our approximation.

Figure 10 is a comparison between the approximation, T-Matrix and the classical Rayleigh. It consists of a calculation of Q_{ext} from a 1.5 aspect ratio, randomly oriented, amorphous carbon, prolate spheroid, at 94 GHz. This could be potentially a part of a model for millimeter-wave propagation through a soot plume. Since both the real and imaginary part of the refractive index ($m = 50 - 50\mathrm{i}$) is very high, the T-Matrix calculation could be unreliable. Indeed, for higher values of b the T-Matrix code will produce negative values of Q_{ext}. Up to about $b = 0.2$ the code is accurate enough for our purposes since the backscatter efficiency and absorption efficiency behave as expected up to this point (when compared

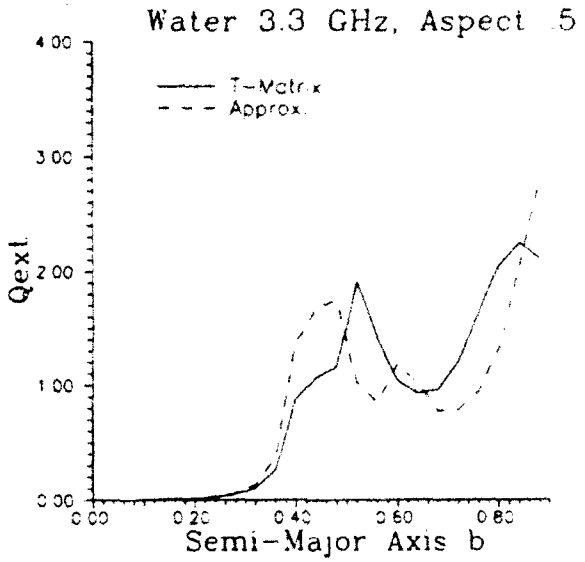

FIGURE 8 – Q_{ext} for water spheroids, r = 0.5, at 3.3 GHz. Refractive index m = 8.743 – 0.6409i.

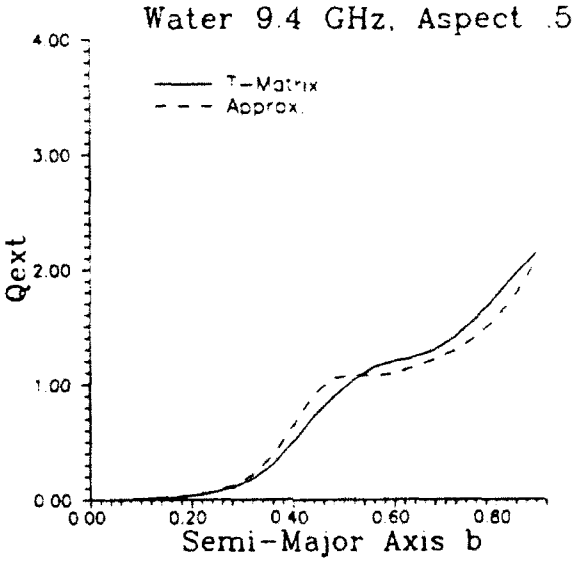

FIGURE 9 – Q_{ext} for water spheroids, r = 0.5, at 9.4 GHz. Refractive index m = 8.075 – 1.824i.

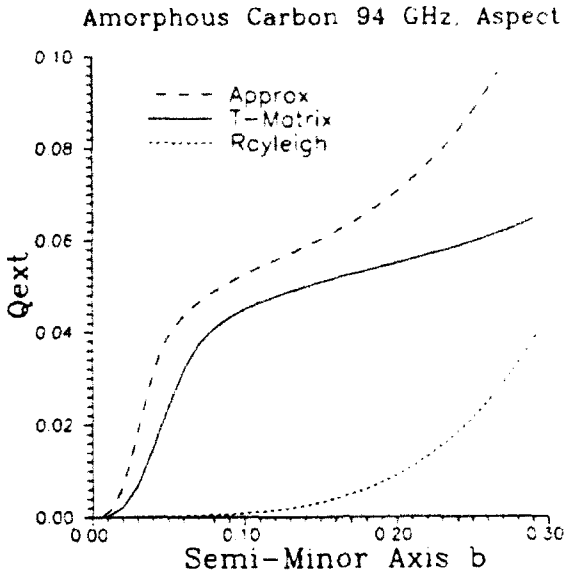

FIGURE 10 – Q_{ext} for amorphous carbon, $r = 1.5$, at 94 GHz. Refractive index $m = 50 - 50i$.

with equivalent volume spheres). It is known that these two efficiencies are more sensitive to numerical instabilities than the extinction efficiency. Keeping this in mind, the new approximation agrees with the T-Matrix calculation to a substantial degree while the classic Rayleigh series does not. This is mainly due to the inclusion of the magnetic dipole terms.

The next example is a model of extinction by randomly oriented copper flakes in the infrared ($m = 35 - 35i$). An oblate spheroid with an aspect ratio of 0.333 was used. For this index, lower aspect ratios could not be considered since the T-Matrix will not produce usable results and hence no comparison could be made. Q_{ext} for this case is shown in Fig. 11. Again, caution is required since the T-Matrix for $b > .25$ begins to decrease rapidly and will go negative, as in the previous case. Again, as in the previous figure, the new

approximation is correct in both form and magnitude as opposed to the Rayleigh series.

As a final example we will use the high-temperature superconductor $YBa_2Cu_3O_{7-\delta}$ at 77 K. For this material and temperature the refractive index can be computed from the model presented in Ref. 9. At 10 GHz we calculate $m = 1.2 - 17683i$. The next three figures, Figs. 12-14, show Q_{ext} for a sphere, an aspect ratio 10 prolate spheroid and an aspect ratio 0.1 oblate spheroid, respectively. As usual, the spheroids are randomly oriented. In the case of the sphere the exact Mie calculation is given. For the spheroids, no exact solution is known. The large deviations from the Rayleigh in all three cases is, as in Fig. 2, ascribable to absorption. Notice that for the largest x shown, Q_{ext} is close to the value predicted by the Rayleigh series. Although it is not clear from these diagrams, Q_{ext} becomes equal to the Rayleigh series, for this range of x, as the eccentricity goes to 1. This is readily seen from [39] and [40] since as $e \to 1$, $L_1 \to 0$ (prolates) or $L_2 \to 0$ (oblates) and $\mathcal{E}_1 \to \infty$ and $\mathcal{U}_1 \to 0$. Thus the electric dipole term dominates the magnetic term. This dominance is the weakest in the case of spheres in which the electric dipole term is only four times the value of the magnetic term (see Fig. 1).

It is evident from the above calculations that it is possible to obtain series for the efficiencies without consideration of optical size, for spheres, spheroids and infinite cylinders. The accuracy of the series for the spheroid would improve if the correct expressions for the spheroidal "Mie" coefficients were used. However, the required spheroidal wave functions

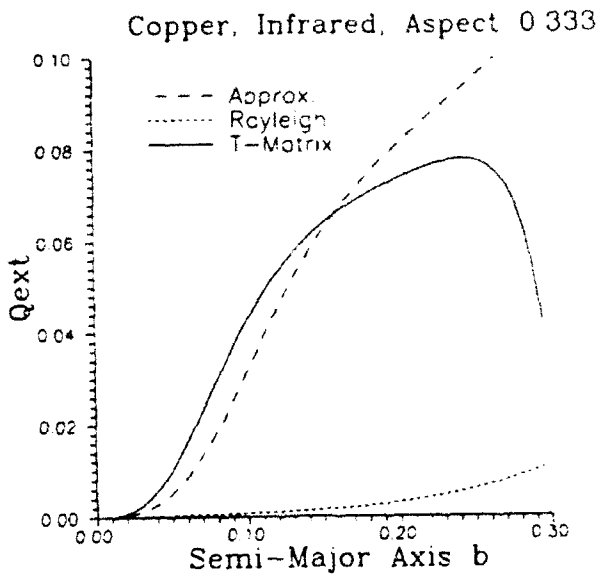

FIGURE 11 – Q_{ext} for copper oblate spheroids, $r = 0.333$, in the infrared. Refractive index $m = 35 - 35i$.

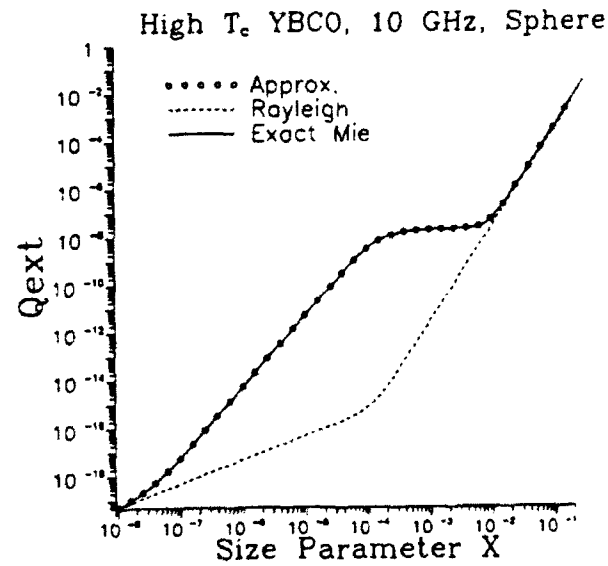

FIGURE 12 – Q_{ext} for spheres of $YBa_2Cu_3O_{7-\delta}$ at 77°K, $r = 1$, at 10 GHz. Refractive index $m = 1.2 - 17683i$.

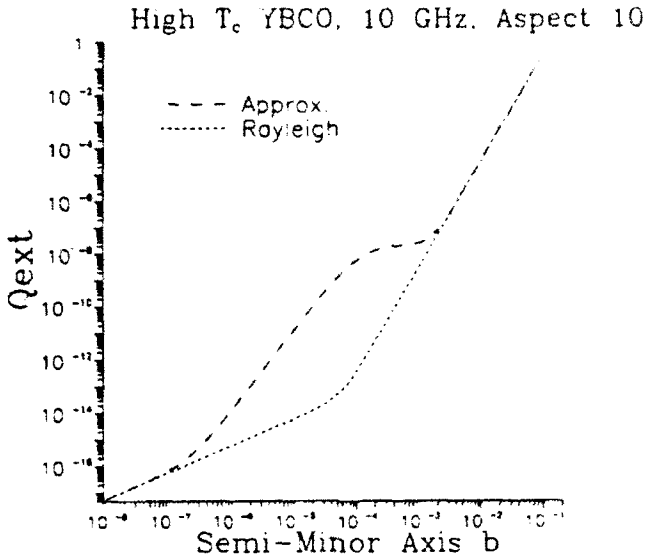

FIGURE 13 – Q_{ext} for spheroids of $YBa_2Cu_3O_{7-\delta}$ at 77°K, $r = 10$, at 10 GHz. Refractive index $m = 1.2 - 17683i$.

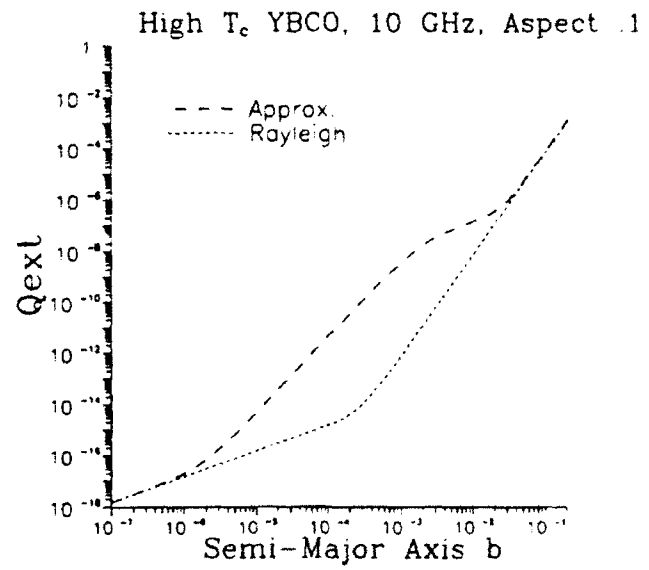

FIGURE 14 – Q_{ext} for spheroids of $YBa_2Cu_3O_{7-\delta}$ at 77°K, $r = 0.1$, at 10 GHz. Refractive index $m = 1.2 - 17683i$.

would lead to complex expressions for $\mathcal{E}_n$ and $\mathcal{U}_n$. Small-particle phase functions can also be computed for arbitrary indices by using the same material transformed series.

4.0 CONCLUSIONS AND REMARKS

We have derived a series that removes the optical size constraint that is inherent in both the Rayleigh and Thomson approximations. This series has been applied to spheres and, in an approximate way, to spheroids. Comparison of the new series with the exact Mie formalism shows excellent agreement. A similar comparison between the T-Matrix method and the randomly oriented spheroid series shows that the agreement is not as good as in the case for spheres. However, a substantial portion of the underlying structure, and hence physics, is being modelled correctly.

Combining this approach with our previously described techniques (Refs. 5 and 10) for approximating extinction, scattering and absorption efficiencies, we have obtained simple formulae for arbitrary materials, particle sizes and aspect ratios. For the first time, estimations of the extinction efficiency for small, highly refractive, elongated, spheroidal particles can be obtained. Since the phase function for small particles is simply related to the first scattering terms, it can also now be obtained for cases that were previously intractable. This gives us the capability to model realistic modern battlefield obscurants as well as radar propagation through rain.

5.0 REFERENCES

1. Van de Hulst, H.C., "Light Scattering by Small Particles", Wiley, New York, 1957.

2. Kerker, M., "The Scattering of Light and Other Electromagnetic Radiation", Academic Press, New York, 1969.

3. Kerker, M., Scheiner, P. and Cooke, D.D., "The Range of Validity of the Rayleigh and Thomson Limits for Lorenz-Mie Scattering", J. Opt. Soc. Am., Vol. 68, pp. 135-137, 1978.

4. Stevenson, A.F., "Electromagnetic Scattering by an Ellipsoid in the Third Approximation", J. Appl. Phys. Vol. 24, No. 9 pp. 1143-1151, 1953.

5. Fournier, G.R. and Evans, B.T.N., "An Approximation to Extinction Efficiency for Randomly Oriented Spheroids", Applied Optics, Vol. 30, pp. 2042-2048, 1991.

6. Barber, P.W., Hill, S.C. and Hill, A.C., "Light Scattering by Size/Shape Distributions of Soil Particles and Spheroids", Applied Optics, Vol. 23, pp. 1025, 1984.

7. Senior, T.B.A., "The Scattering of an Electromagnetic Wave by a Spheroid", Canadian Journal of Physics, Vol. 44, No. 7, pp. 1353, 1966.

8. Asano, S. and Yamamoto, G., "Light Scattering by a Spheroidal Particle", Applied Optics, Vol. 14, pp. 29-49, 1975.

9. Choy, T.C. and Stoneham, A.M., "On the Microwave Loss of Granular High T_c Superconductors in the 0.1 GHz to 1 THz Region", Proc. Royal Society, London A, Vol. 434, pp. 555-570, 1991.

10. B.T.N. Evans and G.R. Fournier, "Simple Approximation to Extinction Efficiency Valid Over All Size Parameters", Applied Optics, Vol. 29, p. 4666-4670, 1990.

INTERNAL DISTRIBUTION

DREV R-4692/93

1 - Deputy Chief
1 - Director Electro-optics Division
1 - Director Energetic Materials Division
6 - Document Library
1 - Dr. B.T.N. Evans (author)
1 - Dr. G.R. Fournier (author)
1 - Dr. P. Pace
1 - Dr. L. Bissonnette
1 - Mr. D. Hutt
1 - Dr. G. Otis
1 - Mr. R. Kluchert
1 - Mr. G. Roy (Energetic Materials)
1 - Mr. G. Couture

EXTERNAL DISTRIBUTION

DREV R-4692/93

2 - DSIS
1 - CRAD
1 - DRDL
1 - DRDM
1 - DMCS
1 - National Library of Canada
1 - Micromedia Limited
1 - NRC/CISTI
1 - DRIC, U.K.
1 - DTIC, U.S.
1 - DISSLB, Australia

1 - Dr. W.G. Tam
Senior Project Manager
Industrial Research Assistance Program
Laboratory Network
National Research Council
Ottawa, Ontario
K1A 0R6

1 - Dr. A.I. Carswell
Dept. of Physics
York University
4700 Keele Street
North York, Ontario
M3J 1P3

1 - Dr. T. Platt
Biological Oceanography Division
Department of Fisheries and Oceans
Bedford Institute of Oceanography
P.O. Box 1006
Dartmouth, N.S. B2Y 4A2

1 - Dr. D. K. Cohoon
West Chester University
Dept. of Mathematics and Computer Science
West Chester, PA, 19383
USA

EXTERNAL DISTRIBUTION (contd)

DREV R-4692/93

1 – Dr. B.P. Curry
NPB Test Stand
Engineering Physics
Argonne National Lab.
9700 South Cass Ave., EP/207
Argonne, IL, 60439-4841
USA

1 – Dr. J. Embury
Chemical Research, Development and Engineering Center
SMCRR-RSP-B
Aberdeen Proving Ground, MD, 21010-5423
USA

1 – Dr. P. Barber
Clarkson College of Technology
Dept. of Electrical & Computer Engineering
Potsdam, NY, 13676
USA

1 – Dr. M. Lax
City College of New York
Physics Dept.
New York, NY, 10031
USA

1 – Dr. R.T. Wang
ISST- Space Astronomy Lab.
1810 NW 6th st.
Gainesville, FL, 32609
USA

1 – Dr. G. Kunz
Physics Laboratory TNO
P.O. Box 9 68 64
2509 The Hague
The Netherlands

EXTERNAL DISTRIBUTION (contd)

DREV R-4692/93

1 - Dr. C.M.P. Platt
CSIRO
Division of Atmospheric Research
Private Bag No. 1, Mordialloc, Vic 3195
Australia